Cell Metabolism
Article

JNK1 in Hematopoietically Derived Cells Contributes to Diet-Induced Inflammation and Insulin Resistance without Affecting Obesity

Giovanni Solinas,[1,2,6] Cristian Vilcu,[3,6] Jaap G. Neels,[3] Gautam K. Bandyopadhyay,[3] Jun-Li Luo,[2] Willscott Naugler,[2] Sergei Grivennikov,[2] Anthony Wynshaw-Boris,[4] Miriam Scadeng,[5] Jerrold M. Olefsky,[3,*] and Michael Karin[2,*]

[1]Laboratory of Metabolic Stress Biology, Division of Physiology, Department of Medicine, University of Fribourg, Chemin du Musée 5, CH-1700 Fribourg, Switzerland
[2]Laboratory of Gene Regulation and Signal Transduction, Department of Pharmacology, School of Medicine
[3]Department of Medicine, Division of Endocrinology and Metabolism
[4]Department of Pediatrics and Department of Medicine
University of California, San Diego, La Jolla, CA 92093, USA
[5]Department of Radiology, University of California, San Diego, San Diego, CA 92098, USA
[6]These authors contributed equally to this work.
*Correspondence: jolefsky@ucsd.edu (J.M.O.), karinoffice@ucsd.edu (M.K.)
DOI 10.1016/j.cmet.2007.09.011

SUMMARY

Obesity-induced insulin resistance is a major factor in the etiology of type 2 diabetes, and Jun kinases (JNKs) are key negative regulators of insulin sensitivity in the obese state. Activation of JNKs (mainly JNK1) in insulin target cells results in phosphorylation of insulin receptor substrates (IRSs) at serine and threonine residues that inhibit insulin signaling. JNK1 activation is also required for accumulation of visceral fat. Here we used reciprocal adoptive transfer experiments to determine whether JNK1 in myeloid cells, such as macrophages, also contributes to insulin resistance and central adiposity. Our results show that deletion of *Jnk1* in the nonhematopoietic compartment protects mice from high-fat diet (HFD)-induced insulin resistance, in part through decreased adiposity. By contrast, *Jnk1* removal from hematopoietic cells has no effect on adiposity but confers protection against HFD-induced insulin resistance by decreasing obesity-induced inflammation.

INTRODUCTION

Type 2 diabetes (T2D) is a common complication of obesity and a sedentary lifestyle (Hu et al., 2001) and a major threat to human health in the 21st century (Zimmet et al., 2001). Although the mechanisms by which increased adiposity contribute to T2D pathogenesis are still being unraveled, it is now well accepted that chronic low-grade obesity-induced inflammatory responses that lead to activation of protein kinases, such as IκB kinases (IKKs) and Jun kinases (JNKs), play an important role in the etiology of this most common metabolic disease (Hotamisligil, 2006; Shoelson et al., 2006; White, 2003). JNK family members are encoded by three genetic loci: the widely expressed *Jnk1* and *Jnk2*, and *Jnk3*, which is mainly expressed in brain and cardiomyocytes (Karin and Gallagher, 2005; Weston and Davis, 2007). JNK1 and JNK2 isozymes have been implicated in obesity-induced glucose intolerance, and JNK1 is believed to be the major contributor (Hirosumi et al., 2002; Tuncman et al., 2006). JNK1 is chronically activated in obesity and T2D, at least in part due to lipotoxic stress (Solinas et al., 2006a; Weston and Davis, 2007). Interference with JNK1 activity by either targeted gene disruption or pharmacological inhibitors protects against obesity-induced insulin resistance (Hirosumi et al., 2002; Kaneto et al., 2004; Tuncman et al., 2006). Since JNK1 is an attractive target for prevention and treatment of T2D and obesity-induced insulin resistance (Kaneto, 2005; Karin, 2005; Manning and Davis, 2003), it is important to fully understand the mechanisms by which it participates in the pathogenesis of glucose intolerance.

Currently, studies on JNK1 action during development of insulin resistance support a common mechanism through which JNK1 activation in insulin target cells directly interferes with insulin signaling (Aguirre et al., 2000, 2002; Hirosumi et al., 2002; Jaeschke et al., 2004; Kaneto et al., 2004; Solinas et al., 2006a; White, 2003). This interference is based on direct phosphorylation of insulin receptor substrates 1 and 2 (IRS1 and IRS2) at inhibitory sites that prevents recruitment to activated insulin receptors (Aguirre et al., 2000, 2002; Solinas et al., 2006a; White, 2003). Thus, JNK-mediated IRS phosphorylation disrupts downstream events such as activation of phosphatidylinositol 3-kinase (PI3K) and AKT (Aguirre et al., 2000, 2002; Lee et al., 2003; Solinas et al., 2006a; White, 2003). Inhibition of JNK1 activation in mouse models of obesity-induced insulin resistance or in cells treated with free fatty acids (FFAs) or inflammatory cytokines results in enhanced insulin-induced PI3K and AKT activation

(Aguirre et al., 2000, 2002; Hirosumi et al., 2002; Jaeschke et al., 2004; Kaneto et al., 2004; Lee et al., 2003; Nguyen et al., 2005; Solinas et al., 2006a).

Studies in *Jnk1*$^{-/-}$ mice have shown that these animals exhibit a remarkable lean phenotype and are largely protected from diet-induced obesity (Hirosumi et al., 2002; Tuncman et al., 2006). In addition to being lean and more insulin responsive, high-fat diet (HFD)-fed *Jnk1*$^{-/-}$ mice exhibit reduced expression of proinflammatory cytokines such as IL-6, TNF-α, IL-12b, MIF, and MCP1 compared to wild-type (WT) mice (Tuncman et al., 2006). These data suggest that JNK1 may also be involved in obesity-induced inflammation. Whether this function and JNK1 activation in cells other than insulin target cells contribute to the pathogenesis of obesity-induced insulin resistance and glucose intolerance is not known. We addressed this question by generating chimeric mice that lack *Jnk1* either in their nonhematopoietic compartment, including all insulin target cells, or only in their hematopoietically derived cells. Our studies show that JNK1 activation in hematopoietically derived cells makes a major contribution to both HFD-induced inflammation and insulin resistance but has no impact on development of obesity per se.

RESULTS

Generation of Mice Lacking *Jnk1* in Either Hematopoietic or Nonhematopoietic Compartments

To determine whether JNK1 in hematopoietically derived cells contributes to obesity-induced inflammation and glucose intolerance, we used adoptive transfer (Janowska-Wieczorek et al., 2001; Senftleben et al., 2001) to generate mice lacking *Jnk1* in either radiation-resistant (nonhematopoietic) or hematopoietically derived cells. WT and *Jnk1*$^{-/-}$ mice were lethally irradiated and reconstituted with either *Jnk1*$^{-/-}$ or WT bone marrow (Figure 1A). Flow cytometry showed that 5 weeks after bone marrow transplantation, white blood cells were efficiently reconstituted and displayed the donor *Jnk1* genotype (Figure 1B). Reconstitution was essentially complete for CD11b^{+} cells (99%), the precursors of macrophages and dendritic cells (Figure 1B). To investigate reconstitution of resident macrophages, we PCR-genotyped different tissues 26 weeks after reconstitution. We detected chimerism in liver and adipose tissue, but not in muscle and brain (Figure 1C). Genotyping of Kupffer cells and parenchymal liver cells indicated that Kupffer cells were almost fully derived from the donor bone marrow, whereas the parenchymal cells were those of the recipient (Figure 1C).

Resistance to Diet-Induced Obesity Is Due to JNK1 Deficiency in the Nonhematopoietic Compartment

Previous studies have shown that *Jnk1*$^{-/-}$ mice are resistant to diet-induced obesity (Hirosumi et al., 2002; Tuncman et al., 2006). To determine the compartment in which JNK1 deficiency prevents obesity, WT and *Jnk1*$^{-/-}$ mice, as well as the bone marrow transplant groups (radiation chimeras), were fed normal chow or HFD for 20 weeks starting at week 6 posttransplantation (Figure 1A). As expected, no differences in body mass were observed in chow-fed mice (data not shown), and *Jnk1*$^{-/-}$ mice on HFD were largely protected from diet-induced obesity (Figure 1D). Importantly, *Jnk1*$^{-/-}$ mice reconstituted with WT bone marrow (*Jnk1*$^{-/-}$+WT-BM chimeras) also were protected from HFD-mediated weight gain and obesity. Magnetic resonance imaging (MRI) after 16 weeks of HFD showed that *Jnk1*$^{-/-}$ mice were much leaner than WT mice and that *Jnk1*$^{-/-}$+WT-BM chimeras were leaner than WT mice reconstituted with *Jnk1*$^{-/-}$ or WT bone marrow (WT+*Jnk1*$^{-/-}$-BM and WT+WT-BM chimeras) (Figures 2A and 2B). Quantification of fat pad volumes by MRI showed that both visceral fat and subcutaneous fat were reduced in *Jnk1*$^{-/-}$ versus WT mice and in *Jnk1*$^{-/-}$+WT-BM versus WT+WT-BM and WT+*Jnk1*$^{-/-}$-BM chimeras (Figures 2A and 2B).

We conclude that resistance to diet-induced obesity in *Jnk1*$^{-/-}$ mice (Hirosumi et al., 2002) is mainly due to *Jnk1* absence from a radiation-resistant cell type of a nonhematopoietic origin.

JNK1 Deficiency in the Nonhematopoietic Compartment Increases Energy Expenditure and Improves Insulin Sensitivity

Jnk1$^{-/-}$ mice have smaller adipocytes than WT mice (Hirosumi et al., 2002), suggesting that decreased adiposity may be due to decreased triglyceride storage rather than reduced adipocyte number. It has also been reported that *Jnk1*$^{-/-}$ mice have normal intestinal lipid uptake and a statistically insignificant tendency toward decreased food intake and increased body temperature (Hirosumi et al., 2002). To better understand the cause of the decreased adiposity, we performed energy balance studies by measuring oxygen consumption and food intake for 60 hr. During this period, we found no differences in food intake between WT and *Jnk1*$^{-/-}$ mice or between the three groups of radiation chimeras (Figures 2C and 2D). However, oxygen consumption per lean body mass was significantly higher in *Jnk1*$^{-/-}$ mice compared to their WT counterparts (Figure 2C). Furthermore, *Jnk1*$^{-/-}$+WT-BM chimeras also exhibited a comparable increase in oxygen consumption relative to WT+WT-BM and WT+*Jnk1*$^{-/-}$-BM chimeras (Figure 2D). These results indicate that resistance to obesity in *Jnk1*$^{-/-}$ and *Jnk1*$^{-/-}$+WT-BM mice is due, at least in part, to increased metabolic rate in a nonhematopoietic cell type.

As expected, *Jnk1*$^{-/-}$ mice maintained for 20 weeks on HFD had improved glucose and insulin tolerance compared to similarly fed WT mice (Figures 3A and 3B). *Jnk1*$^{-/-}$+WT-BM chimeras on HFD also exhibited improved glucose and insulin tolerance compared to similarly fed WT+WT-BM chimeras (Figures 3C and 3D). Moreover, *Jnk1*$^{-/-}$+WT-BM mice displayed lower plasma insulin levels after intraperitoneal injection of 1 g/kg body weight of glucose compared to WT+WT-BM chimeras (see Figure S1 in the Supplemental Data available with this article online).

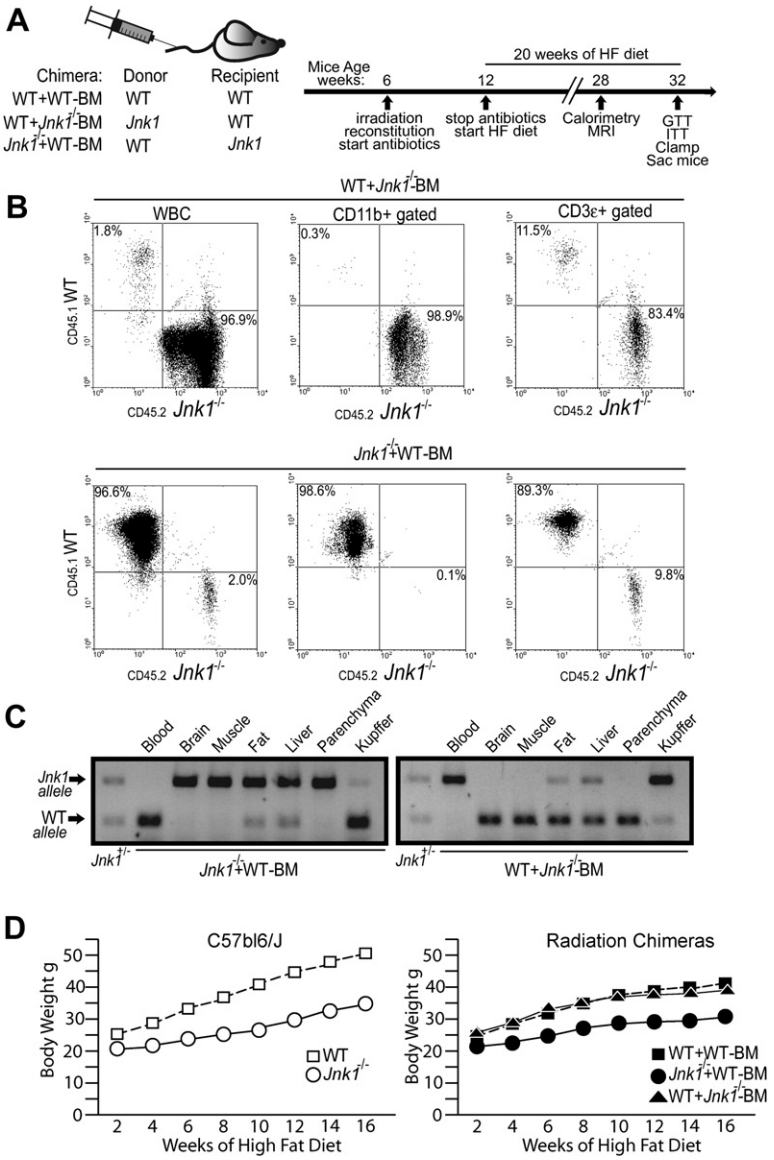

Figure 1. Generation of Hematopoietic and Nonhematopoietic *Jnk1* Knockout Mice

(A) List of radiation chimeras used in this study and experimental design.

(B) Quantification of reconstitution at 5 weeks posttransplantation by flow cytometry of total white blood cells (WBC), $CD11b^+$ cells, and $CD3^+$ cells. $Jnk1^{-/-}$ cells express the CD45.2 (Ly5.1) marker, whereas wild-type (WT) cells express the CD45.1 (Ly5.2) marker.

(C) PCR genotyping of tissues obtained from radiation chimeras 26 weeks after bone marrow transplantation. DNA of $Jnk1^{+/-}$ mice was used as a control (lane 1).

(D) Growth curves of radiation chimeras and WT and $Jnk1^{-/-}$ mice on high-fat diet (HFD).

To better understand the basis for the improved glucose tolerance in $Jnk1^{-/-}$ mice and $Jnk1^{-/-}$+WT-BM chimeras, we performed hyperinsulinemic-euglycemic clamp studies. Although no differences were observed in mice on chow diet (Figure S2), when maintained on HFD, $Jnk1^{-/-}$ mice exhibited higher glucose infusion rates than WT mice (Figure 4A). The increased insulin sensitivity in $Jnk1^{-/-}$ mice was due to both improved insulin-stimulated glucose disposal (Figure 4B) and suppression of hepatic glucose production (Figure 4C). Consistent with the data in Figure 3, we also observed increased insulin sensitivity in $Jnk1^{-/-}$+WT-BM versus WT+WT-BM chimeras ($p < 0.001$) (Figure 4A), and this was due to both improved glucose disposal ($p < 0.001$) (Figure 4B) and enhanced suppression of hepatic glucose production ($p < 0.001$) (Figure 4C).

To investigate the contribution of reduced obesity to improved insulin sensitivity, we performed glucose clamp studies on a group of WT+WT-BM-L chimeras, chimeric mice on HFD that were selected post hoc on the basis of lower body weight than the average for WT+WT-BM chimeras (33.4 g versus 42.1 g body mass), because of a more moderate weight gain during HFD feeding and decreased weight recovery after the clamp surgery. The glucose infusion rate in the WT+WT-BM-L group was significantly higher than in WT+WT-BM chimeras and lower than in $Jnk1^{-/-}$+WT-BM mice, whose average body mass was 28.3 g (Figures 4A). Likewise, WT+WT-BM-L chimeras exhibited improved glucose disposal rate and suppression of hepatic glucose production compared to WT+WT-BM mice (Figures 4B and 4C), whereas compared to the $Jnk1^{-/-}$+WT-BM group, the WT+WT-BM-L chimeras exhibited decreased suppression of hepatic glucose production ($p < 0.05$) and a slightly lower (statistically insignificant; $p = 0.098$) glucose disposal rate (Figures 4B and 4C).

From these results, we conclude that *Jnk1* deletion in the nonhematopoietic compartment protects against diet-induced insulin resistance at least in part because it reduces adiposity.

Absence of *Jnk1* from the Hematopoietic Compartment Improves Insulin Sensitivity in Mice on High-Fat Diet

As described above, *Jnk1* deletion in the hematopoietic compartment does not affect body weight, adiposity, or energy expenditure. Nonetheless, WT+*Jnk1*$^{-/-}$-BM chimeras showed improved glucose and insulin tolerance (Figures 3E and 3F) and a faster decrease in serum insulin following intraperitoneal glucose injection (Figure S1) relative to the WT+WT-BM group. Consistent with this, hyperinsulinemic-euglycemic clamp studies demonstrated that, compared to WT+WT-BM chimeras, WT+*Jnk1*$^{-/-}$-BM mice show improved glucose infusion rate (Figure 4A) due to enhanced insulin-stimulated glucose disposal (Figure 4B) and greater suppression of hepatic glucose production (Figure 4C).

To test whether deletion of *Jnk1* in the hematopoietic compartment improves insulin signaling, we measured insulin-induced AKT phosphorylation in livers of WT+*Jnk1*$^{-/-}$-BM and WT+WT-BM chimeras. The WT+*Jnk1*$^{-/-}$-BM chimeras maintained on HFD showed higher levels of insulin-induced AKT activation compared to WT+WT-BM chimeras maintained on HFD, which were clearly insulin resistant relative to chow-fed counterparts ($p < 0.001$) (Figure 4D; Figure S3).

Absence of *Jnk1* from the Hematopoietic Compartment Decreases Obesity-Induced Inflammation

Jnk1$^{-/-}$ mice show decreased liver expression of proinflammatory cytokine and chemokine mRNAs (IL-6, TNF-α, IL-12b, MIF, and MCP1) relative to WT mice (Tuncman et al., 2006). We assessed whether JNK1 in hematopoietic cells is directly involved in obesity-induced inflammation. Both WT+WT-BM and WT+*Jnk1*$^{-/-}$-BM chimeras on HFD developed hepatosteatosis (Figure S4) and had similar liver triglyceride content (Figure 5A). However, real-time PCR analysis revealed decreased expression of IL-6, TNF-α, IL-12b, MIF, and MCP1, while hepatic expression of the Kupffer cell marker F4/80 in livers of WT+*Jnk1*$^{-/-}$-BM chimeras on HFD was comparable to livers of WT+WT-BM chimeras (Figure 5B; Figure S5A). Similar results, with the exception of MCP1 mRNA, were observed when adipose tissue inflammatory mRNAs were measured (Figure 5D).

Adipose tissue from obese rodents and humans is characterized by increased numbers of resident macrophages, which largely localize around dead adipocytes, forming crown-like structures (CLSs) (Cinti et al., 2005). To enumerate CLSs, we performed MAC2 and 4′,6-diamidino-2-phenylindole (DAPI) staining of adipose tissue sections from WT+WT-BM and WT+*Jnk1*$^{-/-}$-BM chimeras on HFD. The results showed that the number of adipose tissue macrophages in WT+*Jnk1*$^{-/-}$-BM chimeras was less than half ($p < 0.001$) of that in WT+WT-BM chimeras

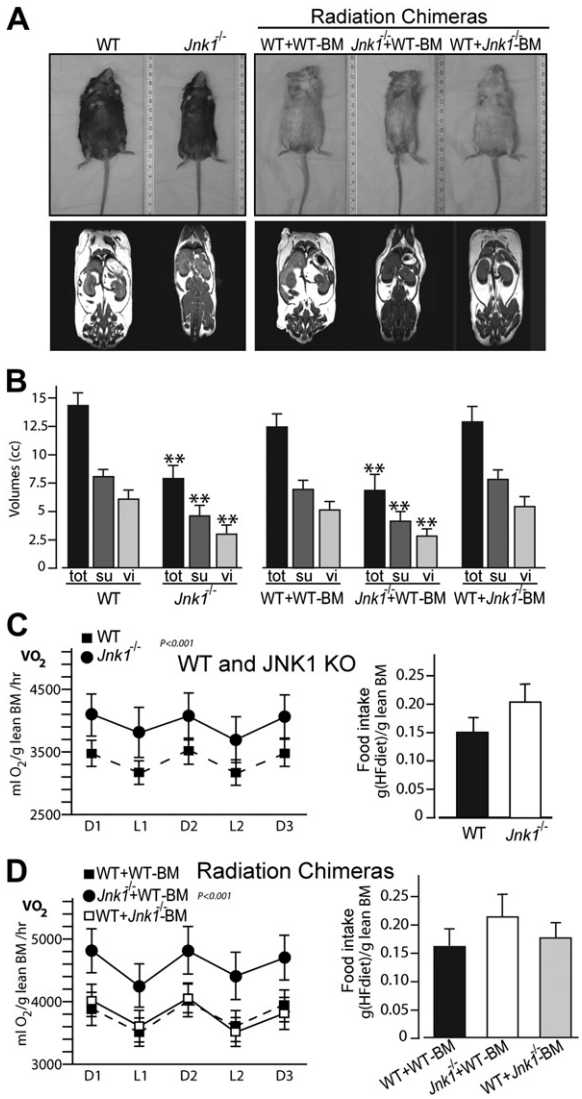

Figure 2. Resistance to Diet-Induced Obesity in *Jnk1*$^{-/-}$ Mice Is Mediated by the Nonhematopoietic Compartment

(A) Representative photographs and MRI images of WT mice, *Jnk1*$^{-/-}$ mice, and radiation chimeras after 16 weeks on HFD.

(B) Quantification of total (tot), subcutaneous (su), and visceral (vi) fat volumes by MRI.

(C) Energy expenditure and food intake of WT and *Jnk1*$^{-/-}$ mice after 16 weeks on HFD. Analysis was performed over three dark (D) and two light (L) cycles of 12 hr each.

(D) Energy balance study performed as described in (C) using the indicated radiation chimeras.

**$p < 0.001$. Error bars represent SD.

(Figure 5C), despite there being no difference in adipocyte size (Figure S6) or chemotactic activity of isolated bone marrow-derived macrophages (Figure S7). Consistent with these observations, real-time PCR analysis demonstrated lower mRNA levels of the macrophage marker F4/80 in adipose tissue from WT+*Jnk1*$^{-/-}$-BM compared to WT+WT-BM chimeras (Figure 5D). However, there were no differences in the total number of peripheral blood

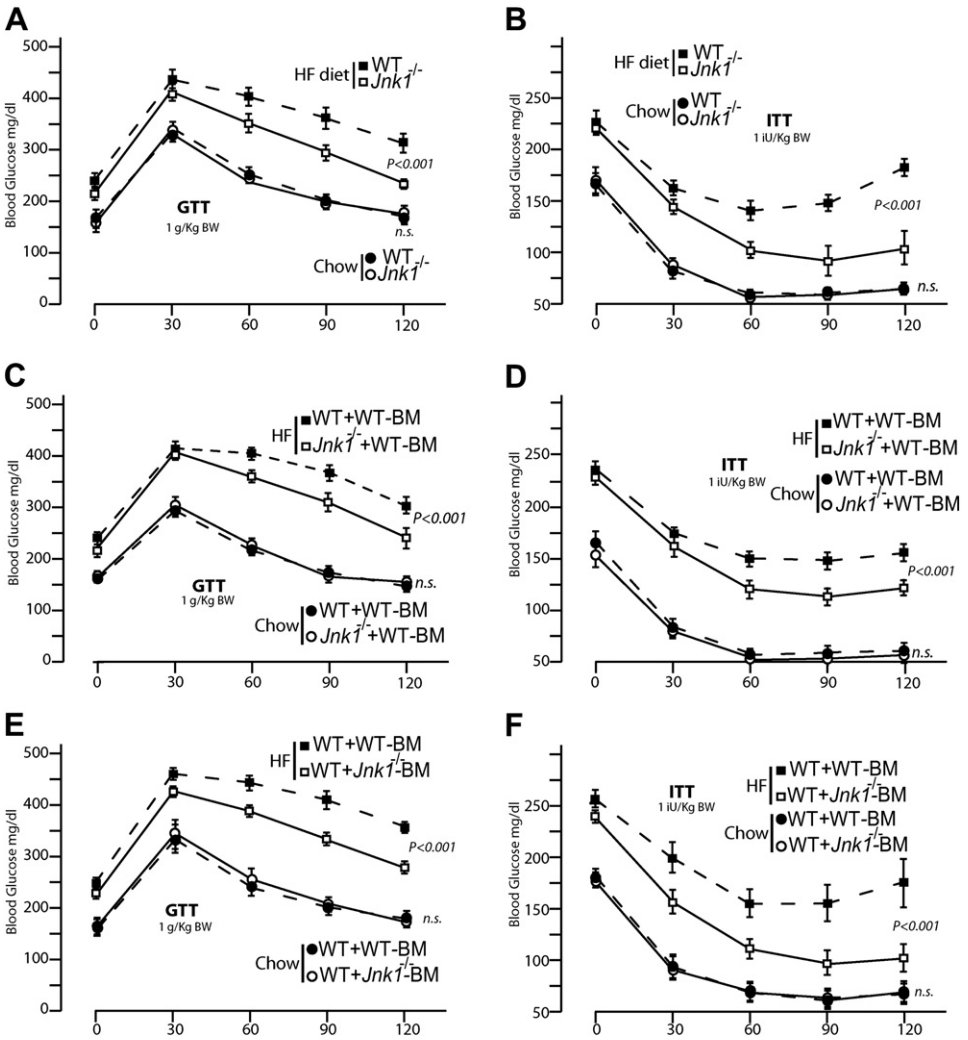

Figure 3. *Jnk1* Deletion in the Nonhematopoietic or Hematopoietic Compartments Improves Glucose and Insulin Tolerance in Response to High-Fat Diet

(A and B) Intraperitoneal glucose tolerance test (GTT) (A) and insulin tolerance test (ITT) (B) of WT and $Jnk1^{-/-}$ mice fed either chow or HFD for 20 weeks.

(C and D) GTT (C) and ITT (D) of WT+WT-BM or $Jnk1^{-/-}$+WT-BM radiation chimeras fed as above.

(E and F) GTT (E) and ITT (F) of WT+WT-BM or WT+$Jnk1^{-/-}$-BM radiation chimeras fed as above.

Error bars represent SEM.

monocytes (PBMs) (Figure S8) or the number of myeloid cells recruited to the peritoneum of WT+$Jnk1^{-/-}$-BM and WT+WT-BM mice injected intraperitoneally with thioglycolate (Figure S9). Therefore, the decreased number of CLSs in WT+$Jnk1^{-/-}$-BM mice is not due to a general defect in macrophage differentiation or recruitment.

To investigate the consequences of reduced adipose tissue inflammation on production of adipokines and FFA release, we measured serum levels of leptin, adiponectin, and FFAs. Although no significant differences in the levels of adipokines between WT+$Jnk1^{-/-}$-BM and WT+WT-BM chimeras were detected, we observed a tendency toward increased adiponectin ($p = 0.061$) and decreased leptin ($p = 0.067$) in WT+$Jnk1^{-/-}$-BM chimeras compared to the WT+WT-BM group (Figure 5F). Interestingly, WT+$Jnk1^{-/-}$-BM mice showed decreased circulating FFA concentrations, suggesting a role for adipose tissue macrophages in lipolysis (Figure 5G). Since lipolysis is inhibited by insulin signaling (Nishino et al., 2007), it is conceivable that the decreased levels of circulating FFAs in WT+$Jnk1^{-/-}$-BM chimeras are consequent to improved insulin signaling in adipose tissue due to decreased inflammation.

JNK1 Is Required for FFA-Mediated Induction of Proinflammatory Cytokines in Macrophages

We have previously proposed that lipotoxic stress from long-chain saturated FFAs is a major cause of JNK activation in obesity (Nguyen et al., 2005; Solinas et al., 2006a). It has also been reported that long-chain saturated FFAs,

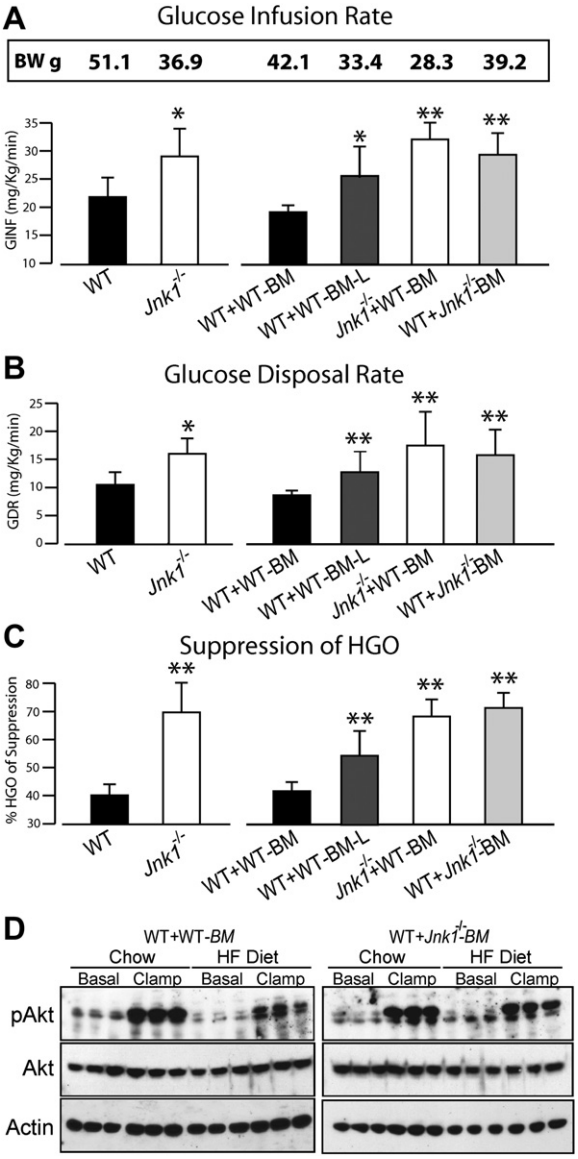

Figure 4. *Jnk1* Deficiency in the Nonhematopoietic or Hematopoietic Compartments Improves Insulin Sensitivity

(A–C) Glucose infusion rate (A), glucose disposal rate (B), and suppression of hepatic glucose production (HGO) (C) of WT mice, *Jnk1*$^{-/-}$ mice, and radiation chimeras maintained on HFD for 22 weeks. Average body weight (BW) of the different groups is indicated at top. *$p < 0.05$; **$p < 0.001$. Error bars represent SD.

(D) AKT phosphorylation was measured in livers collected after the clamp from WT+WT-BM and WT+*Jnk1*$^{-/-}$-BM radiation chimeras fed as above.

but not polyunsaturated FFAs, induce IL-6 and TNF-α in macrophages (Shi et al., 2006). Therefore, we tested whether JNK1 directly regulates expression of proinflammatory cytokines in macrophages exposed to long-chain saturated FFAs. Incubation of peritoneal macrophages with palmitate (PA) caused robust and sustained JNK activation, whereas unsaturated FFAs caused a transient response (Figure 6A; Figure S10). Real-time PCR analysis showed that PA-mediated induction of IL-6 and TNF-α mRNAs was significantly reduced in peritoneal macrophages from *Jnk1*$^{-/-}$ mice (Figure 6B).

Since WT+*Jnk1*$^{-/-}$-BM chimeras maintained on HFD showed improved hepatic insulin signaling compared to WT+WT-BM mice (Figures 4C and 4D), we also tested the role of JNK1 in PA-induced cytokine gene expression in primary Kupffer cells from WT and *Jnk1*$^{-/-}$ mice. As seen in peritoneal macrophages, WT Kupffer cells treated with PA showed sustained JNK activation (Figure 6C) and induction of IL-6 and TNF-α mRNAs, all of which were attenuated in *Jnk1*$^{-/-}$ Kupffer cells (Figure 6D).

To test the effect of PA-induced cytokine expression in macrophages on insulin sensitivity in insulin target cells, we incubated L6 myotubes with conditioned medium from WT peritoneal macrophages treated with PA-loaded BSA, BSA alone, or LPS as a positive control. The results show that conditioned medium harvested from PA- or LPS-treated WT macrophages inhibits insulin-dependent glucose uptake compared to medium from BSA-treated macrophages (Figure 6E; Figure S11). In contrast, conditioned media from PA- or LPS-treated *Jnk1*$^{-/-}$ macrophages did not inhibit insulin-dependent glucose uptake in L6 myotubes.

Together, these results support the hypothesis that JNK1 is an important component of the low-grade inflammatory response triggered by exposure of myeloid cells (macrophages, Kupffer cells, dendritic cells, etc.) to saturated FFAs or other molecules associated with obesity.

DISCUSSION

The currently proposed mechanism for JNK action in obesity-induced insulin resistance involves direct inhibitory phosphorylation of IRS proteins within insulin target tissues such as muscle, liver, and fat (Aguirre et al., 2000, 2002; Hirosumi et al., 2002; Solinas et al., 2006a; White, 2003). JNK-mediated IRS phosphorylation can also inhibit glucose-induced insulin production by pancreatic β cells (Solinas et al., 2006a). The studies described above suggest that JNK1 deficiency protects against diet-induced insulin resistance by at least two additional mechanisms. Absence of *Jnk1* in the nonhematopoietic compartment prevents diet-induced obesity and leads to indirect improvement of insulin sensitivity through maintenance of leaner body mass. By contrast, *Jnk1* deletion in the hematopoietic compartment does not affect adiposity or have a direct effect on insulin receptor signaling but still protects against HFD-mediated insulin resistance by decreasing obesity-induced inflammation. This mechanism may be particularly amenable to therapeutic intervention.

Jnk1-deficient mice maintained on HFD are leaner than WT counterparts, with redistribution of adiposity from subcutaneous to visceral fat, improved insulin sensitivity, and decreased expression of proinflammatory cytokines and chemokines (Hirosumi et al., 2002; Tuncman et al., 2006). We have used reciprocal adoptive transfer experiments to tease apart the different pathophysiological mechanisms through which JNK1 deficiency contributes

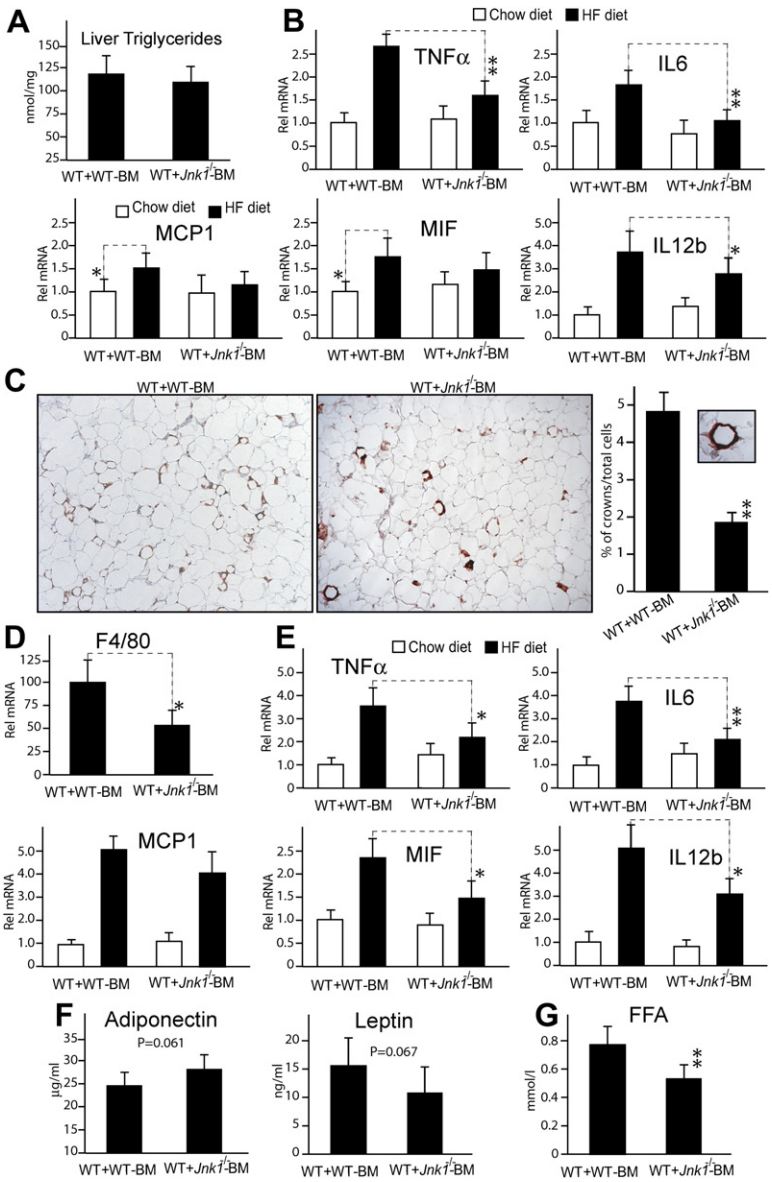

Figure 5. *Jnk1* Deletion in Hematopoietic Cells Decreases Obesity-Induced Inflammation

(A) Liver triglyceride content in WT+WT-BM and WT+*Jnk1*$^{-/-}$-BM radiation chimeras fed a HFD for 22 weeks.

(B) Real-time PCR analysis of cytokine and chemokine mRNA expression in livers of WT+WT-BM and WT+*Jnk1*$^{-/-}$-BM chimeras fed either chow or HFD.

(C) MAC2 staining of adipose tissue sections from the above-described chimeras maintained on HFD and quantification of crown-like structures (CLSs) expressed as a percentage of CLS/total nuclei per field.

(D) Real-time PCR analysis of the macrophage marker F4/80 mRNA in adipose tissue from radiation chimeras maintained on HFD.

(E) Real-time PCR analysis of cytokine mRNAs in adipose tissue from radiation chimeras performed as described in (B).

(F and G) Serum concentrations of adipokines (F) and free fatty acids (G) in mice maintained on HFD.

*$p < 0.05$; **$p < 0.01$. Error bars represent SD.

to these parameters. As previous studies have underscored a role for myeloid cells in the development of insulin resistance by maintaining a chronic, low-grade obesity-triggered inflammatory response (Arkan et al., 2005; Lesniewski et al., 2007; Weisberg et al., 2003), we examined whether JNK1 also acts in the hematopoietic compartment from which myeloid cells are derived. To this end, lethally irradiated mice were reconstituted with bone marrow from different donors and treated with antibiotics to reduce postoperative infection and inflammation (Figure 1A). We also kept these mice on a chow diet for the first 6 weeks after reconstitution before placing them on HFD for 20 weeks. Since HFD was given to younger mice in previous studies (Hirosumi et al., 2002; Tuncman et al., 2006), we studied "unmanipulated" WT and *Jnk1*$^{-/-}$ mice as a reference. We succeeded in reproducing the previously reported improved glucose and insulin tolerance and obesity resistance of *Jnk1*$^{-/-}$ mice, but not the subcutaneous→visceral fat redistribution (Hirosumi et al., 2002), probably due to different experimental conditions. Nonetheless, our results allow dissociation of adipose tissue distribution from obesity-induced inflammation and insulin sensitivity.

We found that *Jnk1*$^{-/-}$+WT-BM chimeras, but not WT+*Jnk1*$^{-/-}$-BM chimeras, gained less weight than controls (Figure 1D), demonstrating that mice lacking *Jnk1* in the nonhematopoietic compartment, but not in hematopoietic derivatives, exhibit reduced adiposity (Figures 2A and 2B). Thus, resistance to obesity is due to absence of *Jnk1* from a nonhematopoietic cell type whose identity remains unknown but could possibly be either the adipocyte itself or a central nervous system component involved in the control of energy balance. In this regard, we observed that mice lacking *Jnk1* in the nonhematopoietic compartment

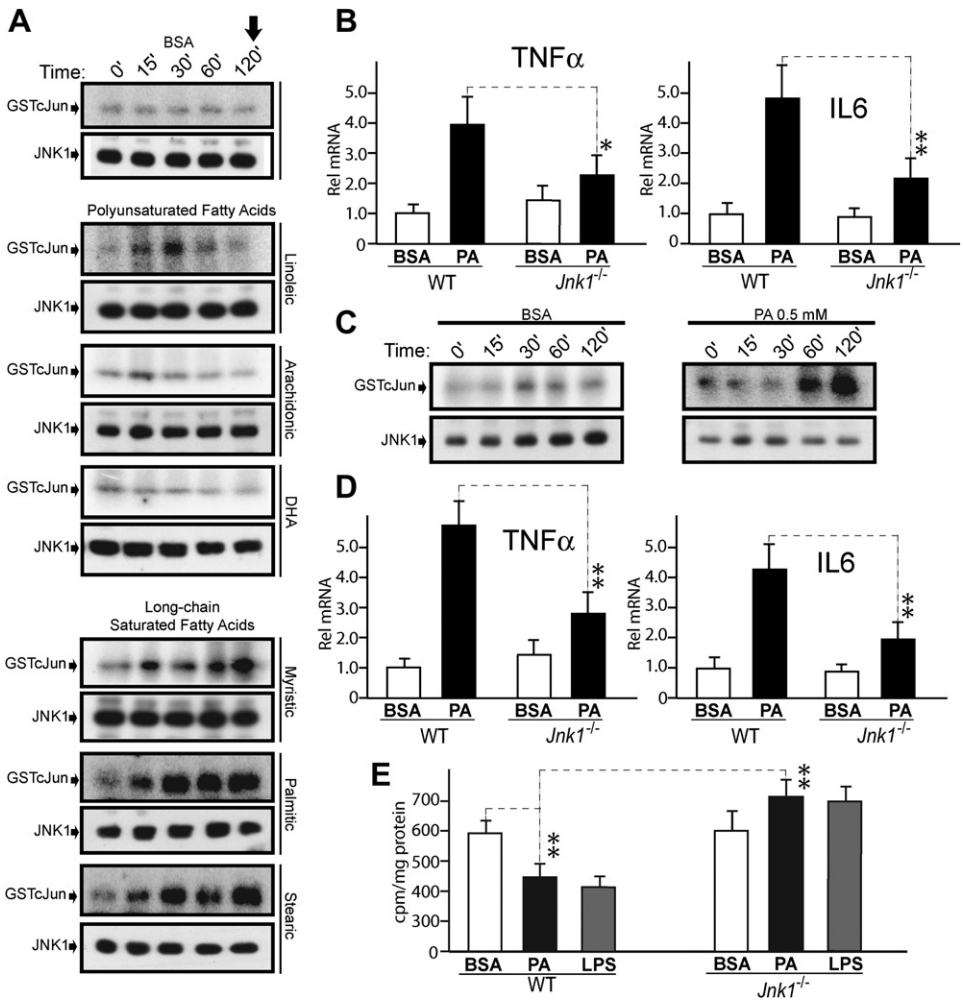

Figure 6. Induction of *TNF-α* and *IL-6* Gene Expression by Palmitate in Macrophages Is JNK Dependent

(A) Solid-state JNK kinase assays using protein extracts from WT peritoneal macrophages. Cells were treated over a 120 min time course with different fatty acid-loaded BSA preparations as indicated. (DHA, *cis*-4,7,10,13,16,19-docosahexaenoic acid.)

(B) Real-time PCR analysis of TNF-α and IL-6 mRNA from WT and *Jnk1*$^{-/-}$ peritoneal macrophages treated with 0.5% BSA or 0.5 mM palmitate (PA) loaded onto 0.5% BSA for 8 hr.

(C) Solid-state JNK kinase assay using protein extracts from Kupffer cells of WT mice. Cells were treated with 0.5% BSA or 0.5 mM PA loaded onto 0.5% BSA for 120 min.

(D) Real-time PCR analysis of TNF-α and IL-6 mRNA from WT and *Jnk1*$^{-/-}$ Kupffer cells treated as in (B).

(E) Insulin-dependent glucose uptake in L6 myotubes incubated with serum-free conditioned media from peritoneal macrophages treated with 0.5% BSA, 0.5 mM PA loaded onto 0.5% BSA, or LPS.

*$p < 0.05$; **$p < 0.01$. Error bars in (B)–(D) represent SD; error bars in (E) represent SEM.

exhibited higher energy expenditure per lean body mass than control mice despite normal food intake. Since no difference in body weight was observed in the chow-fed groups, JNK1 could contribute to obesity by reducing diet-induced thermogenesis in response to HFD, a condition that leads to chronic JNK activation (Hirosumi et al., 2002).

Hyperinsulinemic-euglycemic clamp studies revealed that improved glucose tolerance in *Jnk1*$^{-/-}$ mice is due to enhanced liver and peripheral insulin sensitivity. Improved glucose and insulin tolerance were observed in both *Jnk1*$^{-/-}$+WT-BM and WT+*Jnk1*$^{-/-}$-BM chimeras (Figure 3), and this was also due to enhanced insulin sensitivity in liver and peripheral organs (Figure 4). Comparison of WT+WT-BM chimeras to a leaner group of control chimeras (WT+WT-BM-L) indicated that improved insulin responsiveness in *Jnk1*$^{-/-}$+WT-BM mice is partially due to their obesity-resistant phenotype. These results suggest that pharmacological JNK1 inhibition in nonhematopoietic tissues could protect against the negative effects of HFD by increasing metabolic rate, decreasing adiposity, and improving insulin sensitivity. However, WT+*Jnk1*$^{-/-}$-BM chimeras showed improved insulin sensitivity without an effect on obesity. Thus, the adoptive transfer experiment allowed us to dissociate effects on obesity from effects on insulin resistance in this model,

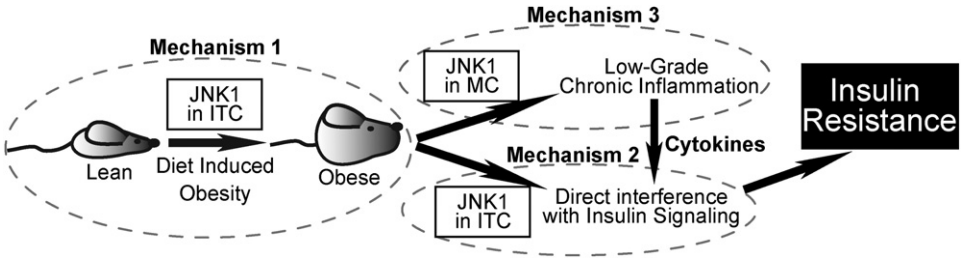

Figure 7. A Model of Our Current Understanding of the Role of JNK1 in Diet-Induced Insulin Resistance

ITC, insulin target cells; MC, myeloid cells. The resistance to diet-induced obesity in *Jnk1*$^{-/-}$ mice is due to nonhematopoietic ITCs (mechanism 1). JNK1 is also directly involved in the development of insulin resistance in ITCs through phosphorylation of IRS1 and IRS2 (mechanism 2) and in MCs by maintaining metabolic inflammation (mechanism 3).

showing that transfer of *Jnk1*$^{-/-}$ hematopoietic cells into WT animals confers an insulin-sensitive phenotype with attenuated HFD-induced inflammatory markers. This observation is fully consistent with a study in which acute JNK inhibition with a specific peptide inhibitor improved liver and peripheral insulin sensitivity in obese mice without affecting body weight (Kaneto et al., 2004).

Obesity triggers a chronic low-grade inflammatory response proposed to promote insulin resistance (Hotamisligil, 2006; Shoelson et al., 2006). Obesity-induced inflammation involves increased expression of proinflammatory cytokines and chemokines and infiltration of macrophages into adipose tissue, where they surround dead adipocytes to form typical CLSs (Cinti et al., 2005). Proinflammatory cytokines in both liver and adipose tissue, as well as the number of CLSs, of HFD-fed mice were reduced upon *Jnk1* deletion in the hematopoietic compartment. Notably, WT+WT-BM and WT+*Jnk1*$^{-/-}$-BM animals on HFD show a comparable increase in hepatic triglycerides and steatosis (Figure 5A; Figure S4), but nevertheless, the WT+*Jnk1*$^{-/-}$-BM animals do not exhibit hepatic insulin resistance (Figure 4C). Since these mice manifest *Jnk1* deletion in Kupffer cells and not in hepatocytes, and since their livers show decreased expression of inflammatory markers (Figure 5B), these results suggest that increased liver triglycerides and steatosis are not sufficient to cause severe hepatic insulin resistance in our model and that the inflammatory response emanating from Kupffer cells is an important cofactor. Correspondingly, we found that JNK1 contributes to cytokine expression in both peritoneal macrophages and Kupffer cells exposed to palmitate and that factors secreted by JNK1-expressing and palmitate-treated peritoneal macrophages induce insulin resistance in cultured myotubes (Figures 6A–6E).

Effects on diet-induced insulin resistance similar to those observed in WT+*Jnk1*$^{-/-}$-BM chimeras were also seen in mice with a conditional knockout in myeloid cells of the proinflammatory kinase IKK and in bone marrow transplantation chimeras for the *Cap* gene (Arkan et al., 2005; Lesniewski et al., 2007). In addition, the effects of PPAR activation on insulin sensitivity are also in part attributed to anti-inflammatory action in myeloid cells (Hevener et al., 2007; Odegaard et al., 2007). At the moment, it is not clear whether JNK1, IKK, Cap, and PPAR control obesity-induced inflammation via a common pathway, but it is now evident that interference with genes involved in macrophage function can protect against HFD-induced insulin resistance by decreasing metabolic inflammation.

At present, we do not know the exact mechanism by which JNK1 inactivation in adipose tissue macrophages decreases CLS formation. However, the facts that *Jnk1*$^{-/-}$ macrophages display normal chemotactic activity in response to adipocyte-conditioned medium (Figure S7) and that WT+*Jnk1*$^{-/-}$-BM chimeras have normal numbers of PBMs and myeloid cells in the peritoneum after thioglycolate injection suggest that the decreased number of CLSs is not due to a defect in PBM chemotaxis. We observed that *Jnk1*$^{-/-}$ macrophages display defective induction of proinflammatory cytokines in response to lipotoxic stress (Figures 6B and 6D), and WT+*Jnk1*$^{-/-}$-BM chimeras showed reduced levels of proinflammatory cytokines in adipose tissue (Figure 5E). Our data therefore suggest that expression of proinflammatory cytokines by adipose tissue macrophages (ATMs) could be required for efficient ATM recruitment into adipose tissue in response to obesity and consequent CLS formation (Figure S12). Since it has been reported that ATMs are composed of at least two different populations of macrophages expressing different markers and with different proinflammatory abilities (Lumeng et al., 2007a, 2007b), it is also plausible that JNK1 could be involved in polarization of ATMs toward the more inflammatory M1 phenotype. Both of these hypotheses imply that CLS formation is a synergistic process in which macrophage activation causes more macrophages to be recruited to adipose tissue, with the end result of increased CLS formation.

Our current understanding of the role of JNK1 in the pathogenesis of obesity-induced insulin resistance is depicted in Figure 7. In summary, JNK activation in a nonhematopoietic cell type allows fat accumulation, perhaps through decreased energy consumption, thereby contributing to insulin resistance via elevated obesity (mechanism 1). As previously described, obesity-induced chronic JNK activation interferes with insulin receptor signaling by inhibiting IRS tyrosine phosphorylation (mechanism 2). In addition, obesity-mediated JNK activation in cells of the hematopoietic compartment promotes obesity-associated inflammation

and production of cytokines or other factors that induce insulin resistance in insulin target cells (mechanism 3). This would represent a two-hit process in which JNK1 in myeloid cells participates in a process causing paracrine activation of JNK1 and decreased insulin signaling in insulin target cells. As myeloid cells could be more accessible to a variety of peptide and small-molecule JNK inhibitors than other cell types, our results suggest that targeting JNK within these cells could make a significant impact in treating insulin resistance.

EXPERIMENTAL PROCEDURES

Radiation Chimeras

Mice were on the C57BL/6 background. To generate radiation chimeras, mice received a lethal dose of 10 Gy of ionizing radiation, followed by tail-vein injection of 10^7 bone marrow cells. To quantify reconstitution efficiency, we used congenic donors and recipients that differed at the *Ly5.1/Ly5.2* locus. Mice were maintained for 6 weeks on chow diet, of which 5 weeks included antibiotics (polymyxin 13 mg/l, neomycin 25 mg/l) to allow bone marrow reconstitution without postoperative infection and inflammation. Mice were placed on HFD 1 week after termination of antibiotic treatment.

Flow Cytometry

Reconstitution efficiency was analyzed by flow cytometric analysis of congenic Ly5.1 (CD45.2-FITC; BD Pharmingen) and Ly5.2 (Cd45.1-PE; BD Pharmingen) markers on blood cells costained for CD3e-PE-Cy5 (eBioscience) or CD11b-Tricolor (Caltag) to identify T cells and monocytes/macrophages, respectively. Whole blood was collected and stained with anti-CD45.2-FITC and anti-CD45.1-PE together with antibodies against T cell or macrophages markers (CD3-CyChrome or CD11b-Tricolor). Cells were washed twice and red blood cells were lysed in ACK buffer (eBioscience). After two additional washes, cells were resuspended in FACS buffer and analyzed via FACSCalibur (BD Biosciences). Data were plotted using WinMDI2.8 software.

PCR Genotyping

Genomic DNA was extracted from tissues or tails by proteinase K digestion (proteinase K 0.5 mg/ml, 100 mM Tris HCl [pH 8.5], 200 mM NaCl, 5 mM EDTA, 0.2% SDS) followed by phenol + chloroform extraction and ethanol precipitation. The following primers were used for *Jnk1* PCR genotyping: forward 5′-CACATACACTCAGTGGATCT-3′; reverse WT 5′-CACTATGTCCTTAAGACTCC-3′; reverse *Jnk1* 5′-TCTT CGCTATTACGCCAGCT-3′.

MRI Analysis and Data Segmentation

After 16 weeks of HFD, lean body mass and fat pad volumes were measured by MRI. Mice were imaged under 1% isoflurane anesthesia in a 5 cm custom volume MRI coil using a horizontal bore 7T MR scanner (GE Medical Systems). Images were acquired using a T1-weighted pulse sequence that rendered fat bright and nonfat tissues dark to facilitate segmentation. Pulse sequence: 2D spin echo sequence TR/TE = 8/300, field of view (FOV) 8 cm, phase FOV 50% with a 320 × 160 matrix, slice thickness 500 μm, 10 averages. This provided an in-plane resolution of 59 μm^3. Image data sets were segmented and volumes were rendered using Amira software (Template Graphic Software/Mercury Computer Systems).

Energy Balance

Oxygen consumption and food intake were measured via Comprehensive Lab Animal Monitoring System (Columbus Instruments). Mice (eight per group) were adapted to metabolic chambers for 2 days before collecting data every 30 min over three dark and two light cycles (12 hr each). At the end of the measurement period, metabolic chambers were inspected for food spillage. Oxygen consumption was normalized per lean body mass measured by MRI.

Glucose and Insulin Tolerance Tests and Hyperinsulinemic-Euglycemic Clamps

Glucose and insulin tolerance tests were performed on 6 hr-fasted mice (Supplemental Experimental Procedures). Blood was collected at 0, 30, 60, 90, and 120 min after intraperitoneal injection, and glucose concentration was measured using an Accu-Check Active glucometer (Roche). For glucose tolerance tests, mice were injected with 1 g/kg body weight of glucose. For insulin tolerance tests, mice were injected with 1 IU insulin/kg body weight. Hyperinsulinemic-euglycemic clamps were performed using 12 mU insulin/kg body weight per minute as previously described (Hevener et al., 2003) (Supplemental Experimental Procedures).

Molecular Measurements

Total RNA was extracted from liver, adipose tissue, or macrophage cell cultures using TRIzol reagent (Invitrogen). cDNA was prepared using a reverse transcription kit (Promega), and quantitative PCR was performed using a commercial SYBR green mix (PE Applied Biosystems) and specific primers for MCP1, IL-12b, MIF, TNF-α, and IL-6 as previously described (Tuncman et al., 2006). *Cph* was used as housekeeping gene control (*Cph* forward 5′-ATGGTCAACCCCACCGTGT-3′; *Cph* reverse 5′-TTCTTGCTGTCTTTGGAACTTTGTC-3′).

For measurement of AKT activation, livers were collected after the clamp experiments, and phospho-AKT Ser473 was quantified as previously described (Solinas et al., 2006b). JNK solid-state kinase assays using GST-cJun(1–79) as a substrate were performed as previously described (Hibi et al., 1993).

Quantification of Crown-Like Structures

Paraffin-embedded epididymal fat pad sections were stained for MAC2 (Cedarlane Labs). Stained slides were subsequently coverslipped with DAPI-containing mounting medium (Vector Labs). Bright-field (MAC2) and fluorescence (DAPI) images were taken of three representative fields per slide in a blinded fashion using a fluorescence microscope (10× objective). Nuclei per field were quantified by counting DAPI-positive nuclei using ImageJ software. MAC2-positive CLSs per field were counted manually, and the percentage of CLSs per total number of nuclei per field was used as a measure of adipose tissue macrophage content (Lesniewski et al., 2007).

Primary Macrophage Cell Culture and Insulin-Stimulated Glucose Uptake in Myotubes

Peritoneal macrophages were isolated from WT or $Jnk1^{-/-}$ mice by peritoneal lavage 4 days after injection of 3 ml of 3% thioglycolate (Difco, BD Diagnostics) and plated in six-well plates at 10^6 cells/well. Kupffer cells were prepared by two-step liver collagenase digestion and fractionation on a Percoll gradient as previously described (Nnalue et al., 1992). The detailed protocol for glucose uptake in L6 myotubes is provided in Supplemental Experimental Procedures.

Statistical Analyses

Differences between two sets of data were compared by Student's t test, and differences over time (GTTs and ITTs) were compared by two-way ANOVA. Differences were considered significant at $p < 0.05$.

Supplemental Data

Supplemental Data include Supplemental Experimental Procedures and 12 figures and can be found with this article online at http://www.cellmetabolism.org/cgi/content/full/6/5/386/DC1/.

ACKNOWLEDGMENTS

G.S. and J.-L.L. generated the radiation chimeras. G.S. performed most of the experiments except for hyperinsulinemic-euglycemic clamps (performed by C.V.), CLS quantification and chemotaxis assay

(performed by J.G.N.), L6 myotube insulin-dependent glucose uptake (performed by G.K.B.), FACS analysis (performed by S.G.), Kupffer cell cultures (prepared by W.N.), oxygen consumption and food intake analysis (performed with the support of A.W.-B.), and MRI studies (M.S.). G.S., J.M.O., and M.K. designed the study and wrote the manuscript.

We thank A.G. Dulloo for advice on the energy balance studies and T. Trang for technical assistance with metabolic cages. G.S. was initially supported by a fellowship from the Swiss National Science Foundation. This research was supported by National Institutes of Health grants ES004151 and ES006376 to M.K. and DK033651 and DK074868 to J.M.O., University of California Discovery Grant #bio06-10567 to J.M.O., and Mentor-Based Postdoctoral Fellowships from the American Diabetes Association to J.M.O. and M.K. M.K. is an American Cancer Society Research Professor.

Received: June 12, 2007
Revised: August 21, 2007
Accepted: September 26, 2007
Published: November 6, 2007

REFERENCES

Aguirre, V., Uchida, T., Yenush, L., Davis, R., and White, M.F. (2000). The c-Jun NH(2)-terminal kinase promotes insulin resistance during association with insulin receptor substrate-1 and phosphorylation of Ser(307). J. Biol. Chem. *275*, 9047–9054.

Aguirre, V., Werner, E.D., Giraud, J., Lee, Y.H., Shoelson, S.E., and White, M.F. (2002). Phosphorylation of Ser307 in insulin receptor substrate-1 blocks interactions with the insulin receptor and inhibits insulin action. J. Biol. Chem. *277*, 1531–1537.

Arkan, M.C., Hevener, A.L., Greten, F.R., Maeda, S., Li, Z.W., Long, J.M., Wynshaw-Boris, A., Poli, G., Olefsky, J., and Karin, M. (2005). IKK-beta links inflammation to obesity-induced insulin resistance. Nat. Med. *11*, 191–198.

Cinti, S., Mitchell, G., Barbatelli, G., Murano, I., Ceresi, E., Faloia, E., Wang, S., Fortier, M., Greenberg, A.S., and Obin, M.S. (2005). Adipocyte death defines macrophage localization and function in adipose tissue of obese mice and humans. J. Lipid Res. *46*, 2347–2355.

Hevener, A.L., He, W., Barak, Y., Le, J., Bandyopadhyay, G., Olson, P., Wilkes, J., Evans, R.M., and Olefsky, J. (2003). Muscle-specific Pparg deletion causes insulin resistance. Nat. Med. *9*, 1491–1497.

Hevener, A.L., Olefsky, J.M., Reichart, D., Nguyen, M.T., Bandyopadyhay, G., Leung, H.Y., Watt, M.J., Benner, C., Febbraio, M.A., Nguyen, A.K., et al. (2007). Macrophage PPAR gamma is required for normal skeletal muscle and hepatic insulin sensitivity and full antidiabetic effects of thiazolidinediones. J. Clin. Invest. *117*, 1658–1669.

Hibi, M., Lin, A., Smeal, T., Minden, A., and Karin, M. (1993). Identification of an oncoprotein- and UV-responsive protein kinase that binds and potentiates the c-Jun activation domain. Genes Dev. *7*, 2135–2148.

Hirosumi, J., Tuncman, G., Chang, L., Gorgun, C.Z., Uysal, K.T., Maeda, K., Karin, M., and Hotamisligil, G.S. (2002). A central role for JNK in obesity and insulin resistance. Nature *420*, 333–336.

Hotamisligil, G.S. (2006). Inflammation and metabolic disorders. Nature *444*, 860–867.

Hu, F.B., Manson, J.E., Stampfer, M.J., Colditz, G., Liu, S., Solomon, C.G., and Willett, W.C. (2001). Diet, lifestyle, and the risk of type 2 diabetes mellitus in women. N. Engl. J. Med. *345*, 790–797.

Jaeschke, A., Czech, M.P., and Davis, R.J. (2004). An essential role of the JIP1 scaffold protein for JNK activation in adipose tissue. Genes Dev. *18*, 1976–1980.

Janowska-Wieczorek, A., Majka, M., Kijowski, J., Baj-Krzyworzeka, M., Reca, R., Turner, A.R., Ratajczak, J., Emerson, S.G., Kowalska, M.A., and Ratajczak, M.Z. (2001). Platelet-derived microparticles bind to hematopoietic stem/progenitor cells and enhance their engraftment. Blood *98*, 3143–3149.

Kaneto, H. (2005). The JNK pathway as a therapeutic target for diabetes. Expert Opin. Ther. Targets *9*, 581–592.

Kaneto, H., Nakatani, Y., Miyatsuka, T., Kawamori, D., Matsuoka, T.A., Matsuhisa, M., Kajimoto, Y., Ichijo, H., Yamasaki, Y., and Hori, M. (2004). Possible novel therapy for diabetes with cell-permeable JNK-inhibitory peptide. Nat. Med. *10*, 1128–1132.

Karin, M. (2005). Inflammation-activated protein kinases as targets for drug development. Proc. Am. Thorac. Soc. *2*, 386–390.

Karin, M., and Gallagher, E. (2005). From JNK to pay dirt: jun kinases, their biochemistry, physiology and clinical importance. IUBMB Life *57*, 283–295.

Lee, Y.H., Giraud, J., Davis, R.J., and White, M.F. (2003). c-Jun N-terminal kinase (JNK) mediates feedback inhibition of the insulin signaling cascade. J. Biol. Chem. *278*, 2896–2902.

Lesniewski, L.A., Hosch, S.E., Neels, J.G., de Luca, C., Pashmforoush, M., Lumeng, C.N., Chiang, S.H., Scadeng, M., Saltiel, A.R., and Olefsky, J.M. (2007). Bone marrow-specific Cap gene deletion protects against high-fat diet-induced insulin resistance. Nat. Med. *13*, 455–462.

Lumeng, C.N., Bodzin, J.L., and Saltiel, A.R. (2007a). Obesity induces a phenotypic switch in adipose tissue macrophage polarization. J. Clin. Invest. *117*, 175–184.

Lumeng, C.N., Deyoung, S.M., Bodzin, J.L., and Saltiel, A.R. (2007b). Increased inflammatory properties of adipose tissue macrophages recruited during diet-induced obesity. Diabetes *56*, 16–23.

Manning, A.M., and Davis, R.J. (2003). Targeting JNK for therapeutic benefit: from junk to gold? Nat. Rev. Drug Discov. *2*, 554–565.

Nguyen, M.T., Satoh, H., Favelyukis, S., Babendure, J.L., Imamura, T., Sbodio, J.I., Zalevsky, J., Dahiyat, B.I., Chi, N.W., and Olefsky, J.M. (2005). JNK and tumor necrosis factor-alpha mediate free fatty acid-induced insulin resistance in 3T3–L1 adipocytes. J. Biol. Chem. *280*, 35361–35371.

Nishino, N., Tamori, Y., and Kasuga, M. (2007). Insulin efficiently stores triglycerides in adipocytes by inhibiting lipolysis and repressing PGC-1alpha induction. Kobe J. Med. Sci. *53*, 99–106.

Nnalue, N.A., Shnyra, A., Hultenby, K., and Lindberg, A.A. (1992). Salmonella choleraesuis and Salmonella typhimurium associated with liver cells after intravenous inoculation of rats are localized mainly in Kupffer cells and multiply intracellularly. Infect. Immun. *60*, 2758–2768.

Odegaard, J.I., Ricardo-Gonzalez, R.R., Goforth, M.H., Morel, C.R., Subramanian, V., Mukundan, L., Eagle, A.R., Vats, D., Brombacher, F., Ferrante, A.W., and Chawla, A. (2007). Macrophage-specific PPARgamma controls alternative activation and improves insulin resistance. Nature *447*, 1116–1120.

Senftleben, U., Li, Z.W., Baud, V., and Karin, M. (2001). IKKbeta is essential for protecting T cells from TNFalpha-induced apoptosis. Immunity *14*, 217–230.

Shi, H., Kokoeva, M.V., Inouye, K., Tzameli, I., Yin, H., and Flier, J.S. (2006). TLR4 links innate immunity and fatty acid-induced insulin resistance. J. Clin. Invest. *116*, 3015–3025.

Shoelson, S.E., Lee, J., and Goldfine, A.B. (2006). Inflammation and insulin resistance. J. Clin. Invest. *116*, 1793–1801.

Solinas, G., Naugler, W., Galimi, F., Lee, M.S., and Karin, M. (2006a). Saturated fatty acids inhibit induction of insulin gene transcription by JNK-mediated phosphorylation of insulin-receptor substrates. Proc. Natl. Acad. Sci. USA *103*, 16454–16459.

Solinas, G., Summermatter, S., Mainieri, D., Gubler, M., Montani, J.P., Seydoux, J., Smith, S.R., and Dulloo, A.G. (2006b). Corticotropin-releasing hormone directly stimulates thermogenesis in skeletal muscle possibly through substrate cycling between de novo lipogenesis and lipid oxidation. Endocrinology *147*, 31–38.

Tuncman, G., Hirosumi, J., Solinas, G., Chang, L., Karin, M., and Hotamisligil, G.S. (2006). Functional in vivo interactions between JNK1 and JNK2 isoforms in obesity and insulin resistance. Proc. Natl. Acad. Sci. USA *103*, 10741–10746.

Weisberg, S.P., McCann, D., Desai, M., Rosenbaum, M., Leibel, R.L., and Ferrante, A.W., Jr. (2003). Obesity is associated with macrophage accumulation in adipose tissue. J. Clin. Invest. *112*, 1796–1808.

Weston, C.R., and Davis, R.J. (2007). The JNK signal transduction pathway. Curr. Opin. Cell Biol. *19*, 142–149.

White, M.F. (2003). Insulin signaling in health and disease. Science *302*, 1710–1711.

Zimmet, P., Alberti, K.G., and Shaw, J. (2001). Global and societal implications of the diabetes epidemic. Nature *414*, 782–787.